Journal of Biomedical Optics

BiomedicalOptics.SPIEDigitalLibrary.org

Safety of cornea and iris in ocular surgery with 355-nm lasers

Jenny Wang
Jae Lim Chung
Georg Schuele
Alexander Vankov
Roopa Dalal
Michael Wiltberger
Daniel Palanker

SPIE.

Safety of cornea and iris in ocular surgery with 355-nm lasers

Jenny Wang,[a,*] Jae Lim Chung,[b,c] Georg Schuele,[d] Alexander Vankov,[d] Roopa Dalal,[b] Michael Wiltberger,[d] and Daniel Palanker[b,e]
[a]Stanford University, Department of Applied Physics, 452 Lomita Mall, Stanford, California 94305, United States
[b]Stanford University, Department of Ophthalmology, 452 Lomita Mall, Stanford, California 94305, United States
[c]Konyang University, Kim's Eye Hospital, Department of Ophthalmology, 136 Yeongshin-ro, Youngdeungpo-gu, Seoul 150-034, Republic of Korea
[d]Abbott Medical Optics, 1310 Moffett Park Drive, Sunnyvale, California 94089, United States
[e]Stanford University, Hansen Experimental Physics Laboratory, 452 Lomita Mall, Stanford, California 94305, United States

Abstract. A recent study showed that 355-nm nanosecond lasers cut cornea with similar precision to infrared femtosecond lasers. However, use of ultraviolet wavelength requires precise assessment of ocular safety to determine the range of possible ophthalmic applications. In this study, the 355-nm nanosecond laser was evaluated for corneal and iris damage in rabbit, porcine, and human donor eyes as determined by minimum visible lesion (MVL) observation, live/dead staining of the endothelium, and apoptosis assay. Single-pulse damage to the iris was evaluated on porcine eyes using live/dead staining. In live rabbits, the cumulative median effective dose (ED_{50}) for corneal damage was 231 J/cm^2, as seen by lesion observation. Appearance of endothelial damage in live/dead staining or apoptosis occurred at higher radiant exposure of 287 J/cm^2. On enucleated rabbit and porcine corneas, ED_{50} was 87 and 52 J/cm^2, respectively, by MVL, and 241 and 160 J/cm^2 for endothelial damage. In human eyes, ED_{50} for MVL was 110 J/cm^2 and endothelial damage at 453 J/cm^2. Single-pulse iris damage occurred at ED_{50} of 208 mJ/cm^2. These values determine the energy permitted for surgical patterns and can guide development of ophthalmic laser systems. Lower damage threshold in corneas of enucleated eyes versus live rabbits is noted for future safety evaluation. [DOI: 10.1117/1.JBO.20.9.095005]

Keywords: ultraviolet laser damage; cornea; iris; eye safety; laser surgery.

Paper 150339R received May 19, 2015; accepted for publication Aug. 3, 2015; published online Sep. 11, 2015.

1 Introduction

Laser-assisted *in situ* keratomileusis (LASIK) is the most common refractive surgery in the United States, with over 600,000 procedures/year. The first step in LASIK is the cutting of a thin corneal flap, which is peeled back to expose the stroma for reshaping by excimer laser ablation. Initially, mechanical microkeratomes were used to create the corneal flap but infrared femtosecond laser systems,[1] which can cut thinner, more precise, and customizable flaps,[2] were soon developed. Despite the increased cost compared to microkeratomes, femtosecond laser systems have become the most common choice for corneal flap creation.[3]

Recently, a promising new laser system for corneal flap cutting that uses a subnanosecond microchip ultraviolet (UV) laser has been demonstrated.[4,5] The simpler design of the 355-nm laser offers a much more compact, inexpensive, and precise flap cutter than is possible with current femtosecond lasers. However, the transition from near-infrared to UV wavelength presents new safety hazards that must be considered before clinical use. Although the 2013 study by Trost et al.[4] showed that 6.5-mm diameter corneal flaps could be created in rabbits with no unintended UV-induced damage to the cornea at a total radiant exposure of 6.9 J/cm^2, it did not establish an operational range and safety margin for 355-nm lasers. A measurement of the actual damage thresholds is important to establish the safety limits of 355-nm lasers for the full range of flap cutting parameters as well as other potential applications, such as refractive lenticule extraction,[6] lamellar keratoplasty,[7] or cataract surgery.[8]

Of the three major damage mechanisms for any laser ocular surgery, photomechanical, photothermal, and photochemical, we are mostly concerned with photochemical damage for 355-nm lasers as it sets a hard limit on the total energy that can be delivered during a procedure. Photomechanical damage is induced by microexplosions during dielectric breakdown-based laser cutting of the stroma and was shown to be lower with 355-nm nanosecond laser than with 1053-nm wavelength and femtosecond pulse durations.[4,5] Therefore, it is reasonable to assume that laser procedures that are within the photomechanical safety limits for near-infrared femtosecond lasers will not produce additional mechanical damage in 355-nm subnanosecond laser systems. Photothermal damage to ocular tissues may arise from cumulative heating, but that can be mitigated by external cooling of the corneal surface or by reducing the average laser power, albeit at the expense of extended duration of the surgical procedure. The photochemical damage threshold is the critical value because UV lasers, unlike infrared lasers, have sufficiently high photon energy to interact linearly with biomolecules. Thus, the photochemical threshold determines

*Address all correspondence to: Jenny Wang, E-mail: jywang2@stanford.edu

the maximum total energy that can be safely deposited in ophthalmic procedures performed with a 355-nm laser.

In this study, we determine the photochemical damage threshold on the cornea because it is most sensitive to damage at 355 nm. Unlike near-infrared laser light, 355 nm is significantly absorbed in the cornea and crystalline lens. According to aggregated data and fits by Kraats and Norren,[9] the average transmission of the cornea is 60% for 355 nm, while the lens transmits <0.3% of the remaining radiation. This protects the retina from damage during laser treatment and means that clinical use of UV lasers is limited by cytotoxicity to the cornea and lens. We focus on the cornea because it was shown in studies by Pitts et al.[10] and Zuclich[11] to have a lower photochemical damage threshold than the lens.

Several previous studies provide valuable guidance for the corneal damage threshold at UVA wavelengths (315 to 400 nm). A 1977 study by Pitts et al.[10] with pigmented rabbits measured the damage threshold at 335 and 365 nm to be 10.99 and 42.5 J/cm^2, respectively. Another study by Zuclich and Connolly[12] with rhesus monkeys determined a damage threshold of 66 J/cm^2 for 350.7-nm/356.4-nm light (3:1 ratio). While these are close to the 355-nm wavelength of interest, the rapidly changing photosensitivity in this wavelength range means that determining the value at the precise wavelength of interest remains important. Here, we measure the photochemical threshold of corneal damage in live rabbits and in enucleated eyes from rabbit, pig, and human after exposure to a subnanosecond microchip 355-nm laser. Visible lesion observation in a slit lamp, live/dead staining, and terminal deoxynucleotidyl transferase dUTP nick-end labeling (TUNEL) assay for apoptosis are compared as complimentary damage assessment methods. We also investigate the effect of two common topical anesthetics, tetracaine and proparacaine, on the damage threshold in enucleated pig eyes.

Thermal damage to the iris due to cumulative heating by near-infrared femtosecond laser during LASIK flap creation was ruled out in a study by Sun et al.[13] UV nanosecond laser systems may be slightly more susceptible to iris damage from cumulative laser heating due to the increased absorption of UV radiation in the iris and decreased reflectivity compared to near-infrared.[14] Nevertheless, thermal damage can be avoided by reducing the average power and extending the procedure. Instead, we consider the possibility of iris damage with single subnanosecond laser pulses if they are focused into sufficiently small spots to cause explosive vaporization of melanosomes.[15] This may occur with patterns that come very close to the limbus or due to error in focusing. The only laser safety standard (ANSI Z136.1) addressing iris exposure is not based on experimental data but on extrapolation from corresponding skin threshold. Here, we measure the single-pulse iris damage threshold by using live/dead staining to visualize the cell death caused by 355-nm laser pulses in enucleated porcine eyes.

2 Methods

2.1 *Laser Setup*

Two similar microchip seeded frequency-tripled Nd:YVO_4 subnanosecond lasers were used in this study. Most of the corneal exposures were performed with a 100-mW, 30-kHz, 355-nm, and 0.55-ns laser (Helios, Coherent, Santa Clara, CA) in one of two configurations. The small beam configuration shown in Fig. 1(a) uses a singlet lens to create a Gaussian profile with $1/e^2$ diameter of 0.87 mm at the sample plane. The larger beam configuration in Fig. 1(b) uses an 800 μm pinhole positioned within a telescope to obtain an apertured Gaussian profile with 1.4-mm beam diameter. This arrangement provided sharp beam edges, which help in detecting lesion margins. The beam profiles were measured with a BeamGage camera (Ophir Optronics, Jerusalem, Israel) and the time-averaged spatial peak irradiances were calculated to be 26.6 W/cm^2 for the small beam at the average power of 80 mW used in experiments and 5.0 W/cm^2 for the larger apertured beam with 40 mW of power. In both configurations, the power could be adjusted using a half-wave plate and polarizing beam splitter while the exposure duration was controlled via electronic shutter. A scanning mirror was used to place patterns of up to 18 spots on the cornea. Cumulative radiant exposure was varied between spots in a pattern by changing the exposure duration while the average power was kept constant. The intersection of two visible diode lasers (Coherent, Santa Clara, California) was used to define the treatment plane and pattern center for alignment of the eye.

The second laser, a 20-mW, 1-kHz, 355-nm, and 0.8-ns laser (PowerChip PNV, Teem Photonics, France), was used in one of two configurations for initial exposures of porcine corneas [Fig. 1(c)] and for single-pulse iris damage experiments [Fig. 1(d)]. Here, the power could be adjusted using a half-wave plate and Brewster angle polarized beam splitter, and exposures were set via electronic shutter. For initial porcine cornea testing, a lens was used to collimate the laser output with $1/e^2$ diameter of 1.1 mm. The beam was kept fixed and spot patterns were delivered by moving the sample via translation stage between exposures. At the experimental average power of 15 mW, the time-averaged spatial peak irradiance on the cornea was 3.2 W/cm^2. As in previous setups, the cumulative radiant exposure was varied by changing laser exposure duration via the electronic shutter. For iris testing, the collimated output beam was loosely focused to a 60 μm spot and a scanning mirror (Optics in Motion, Long Beach, California) driven by a function generator was used to separate the laser pulses on the iris into individual spots. Here, the laser pulse energy was directly varied to determine the single-pulse threshold. Two intersecting He–Ne beams (JDS Uniphase, Milpitas, California) were used for iris sample alignment to the focal plane.

2.2 *Corneal Damage in Enucleated Eyes*

Ex vivo eyes from New Zealand white rabbits ($n = 24$), pigs ($n = 68$), and humans ($n = 6$) were obtained for this study. Porcine eyes (First Vision Tech, Sunnyvale, Texas) were enucleated by the abattoir and shipped overnight on ice in a saline solution. Rabbit eyes (Animal Technologies, Tyler, Texas) were kept in the head and shipped overnight on ice where they were enucleated shortly before to laser exposure. Human eyes were obtained from the San Diego Eye Bank and also shipped overnight on ice. In all cases, eyes were removed from ice between 5 and 10 min before lasering and checked to ensure corneal clarity. The corneal surface was generally between 10 and 15 °C at the start of lasering and warmed to room temperature over the course of the laser exposure. The eye was pinned to a styrofoam base for laser delivery and aligned to the laser pattern center using the aiming beams. The tissue was wetted with several drops of balanced salt solution (BSS) before and after lasering. For pig eyes used to study the effect of topical anesthetics, BSS was replaced by either proparacaine (0.5%,

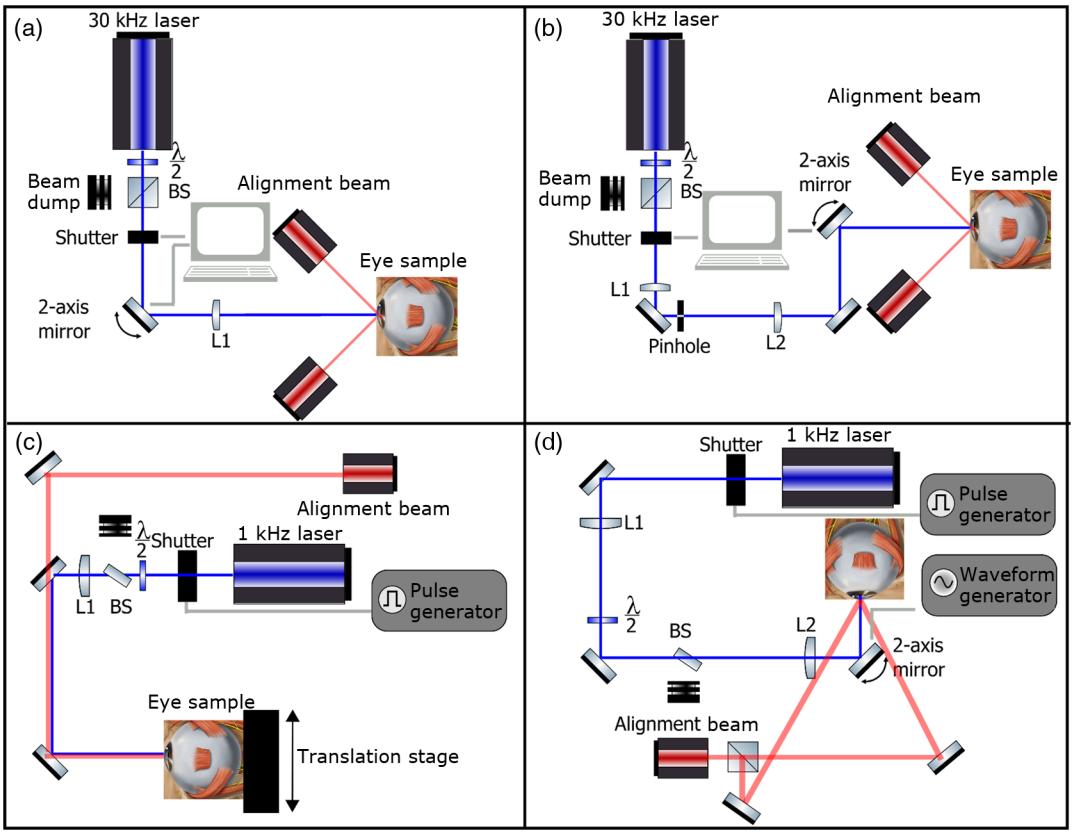

Fig. 1 Laser setups. (a) 30-kHz laser setup in small beam (0.87 mm) configuration (b) 30-kHz laser setup in apertured large beam (1.4 mm) configuration (c) 1-kHz laser setup for corneal exposures with 1.1-mm beam, and (d) 1-kHz laser setup for iris exposures with focused spot of 60 μm.

Bausch & Lomb, Tampa, Florida) or tetracaine (0.5%, Bausch & Lomb) and care was taken to ensure that the drops were added ~5 min before laser exposure. A 3 × 3 grid of laser spots (2 mm center-to-center spacing) was delivered with total irradiation times between 5 and 20 min.

A surgical marking pen was used to outline the lasered area and indicate orientation. After laser exposure, the eyes were wrapped in saline-soaked gauze and kept for 24 h in closed jars at room temperature before analysis. Determination of the minimum visible lesion (MVL) was done by examination under illumination or with a slit lamp. In general, the cornea was slightly cloudier 24 h after laser delivery but laser lesions could be detected as more severe and localized opacities. For nonpigmented New Zealand white rabbit eyes, a small amount (~0.2 mL) of toluidine blue was injected into the vitreous to increase lesion visibility.

Endothelial damage was assessed by live/dead staining. A 30G needle was used to inject 0.3 mL (rabbit and human eyes) or 0.5 mL (porcine eyes) of calcein AM (4 μM)/EthD-III (16 μM) stain (Viability/Cytotoxicity Kit, Biotium, Hayward, California) into the anterior chamber of the eye. After 20 min incubation with the stain, ~0.15 mL of 10% formalin was injected into anterior chamber to stabilize the corneal endothelium. The cornea was removed from the eye after 5 min of formalin fixation. To enhance identification of endothelial cell boundaries, several drops of 0.5% alizarin red dye were placed on the endothelial side of the corneal sample and rinsed off with saline after 2 min. Extraneous cornea was cut off from the laser area with a razor blade to reduce the curvature of the sample before imaging with fluorescence microscopy. Selected porcine corneas were fixed overnight in 10% formalin without live/dead staining, embedded in paraffin, and sectioned. A TUNEL assay (DeadEnd Fluorometric TUNEL, Promega, Wisconsin) to detect apoptosis was performed according to manufacturer instructions, and 4',6-diamidino-2-phenylindole (DAPI) staining (Vectashield, Vector Labs, Burlingame, California) was added to identify cell nuclei in fluorescence microscopy.

2.3 *Corneal Damage in Rabbits*

A total of 12 Dutch-belted rabbits (24 eyes) were used in accordance with the Association for Research in Vision and Ophthalmology Resolution on the Use of Animals in Ophthalmic and Vision Research, with approval from the Stanford University Animal Institutional Review Board. The rabbits were anesthetized for laser delivery and slit lamp observation using ketamine hydrochloride (35 mg/kg) and xylazine (5 mg/kg). The pupil was dilated using one drop each of 1% tropicamide and 2.5% phenylephrine hydrochloride. Several drops of topical tetracaine hydrochloride 0.5% were used for local anesthesia. An ocular speculum was inserted to ensure the eye remained open during laser treatment and saline drops were added periodically to prevent epithelial damage from drying. The head was positioned so that the eye was aligned with the crossed aiming beams and a 3 × 3 pattern of spots (2-mm center spacing) was delivered. Total irradiation time varied between 10 and 25 min.

After irradiation, rabbits were examined by slit lamp at predetermined time points: 1, 12, 48 h and 1, 2, and 4 weeks. The

appearance of visible lesions was noted as an indication of corneal damage. The corneal endothelium was analyzed at either 12 or 48 h after laser treatment by live/dead staining as described above for enucleated eyes. For apoptosis detection, identical patterns were delivered to the left and right eyes. The rabbit was euthanized 12 h after laser irradiation and one eye was taken for live/dead analysis while the other was fixed immediately in 10% formalin for the TUNEL assay (DeadEnd Fluorometric TUNEL, Promega, Wisconsin).

2.4 *Iris Damage in Enucleated Porcine Eyes*

Iris damage was assessed using 21 enucleated porcine eyes with dark pigmentation. Prior to laser exposure, the cornea was cut off and the iris surface was aligned to the focus of the laser delivery system. Marker lines were delivered with high energy and slower scanning, so the 10-μJ pulses would overlap, creating lines of damage visible to the naked eye. Between these marker lines, up to five regularly spaced lines of separated pulses were made with various pulse energies. Immediately after irradiation, the iris was cut out of the eye and soaked for 20 min in calcein AM (2 μM)/ethidium homodimer (4 μM) stain. The iris anterior surface layer was then imaged with fluorescence microscopy.

3 Results

3.1 *Corneal Damage Threshold in Enucleated Eyes*

Irradiated corneas of enucleated eyes were analyzed 24 h after the laser pattern [Fig. 2(a)] delivery by observation in slit lamp or under illumination from surgical microscope. Laser damage was seen as opacities of varying intensity or vacuoles and defects in the epithelium. Figures 2(b) and 2(c) show examples of laser-induced opacities in porcine and rabbit eye, respectively. Viewing the corneas at large angles to the illumination source made the lesions more apparent, particularly for lesions near the threshold. Each lesion was given a damage or no-damage grade and any visible opacity or epithelial change was considered to be damage.

Endothelial damage was determined after staining with live/dead fluorescent assay in which live cells are labeled with a cytoplasmic green fluorescent dye (calcein AM) and dead cells are labeled with red fluorescent dye (EthD-III) in the nuclei. For laser lesions that were far above threshold, nearly every cell has bright red stained nuclei, as shown in Fig. 2(d). For threshold determination, any endothelial changes were graded as damage. An example of subtle damage on the porcine endothelium is shown in Fig. 2(e): several unlabeled (dark) cells (*) can be seen in the center; enlarged cells with increased green fluorescence can be seen at the lesion edge (#). The collected statistics of damage from laser treatment of enucleated porcine and rabbit eyes were fit using probit analysis and shown in Fig. 3 with shaded areas representing the 95% fiducial limits. The median effective dose (ED_{50}) values for MVL appearance were 52 and 87 J/cm^2 in porcine ($n = 393$ laser spots) and rabbit ($n = 183$ laser spots) eyes, respectively. Endothelial damage ED_{50} values were 160 and 241 J/cm^2 for porcine ($n = 233$ laser spots) and rabbit ($n = 183$ laser spots) eyes. Human donor eyes were analyzed in the same way, with lesion observation followed by staining of the endothelium. Probit analysis yielded ED_{50} values of 110 and 453 J/cm^2 for MVL ($n = 52$ laser spots) and endothelial damage ($n = 45$ laser spots), respectively.

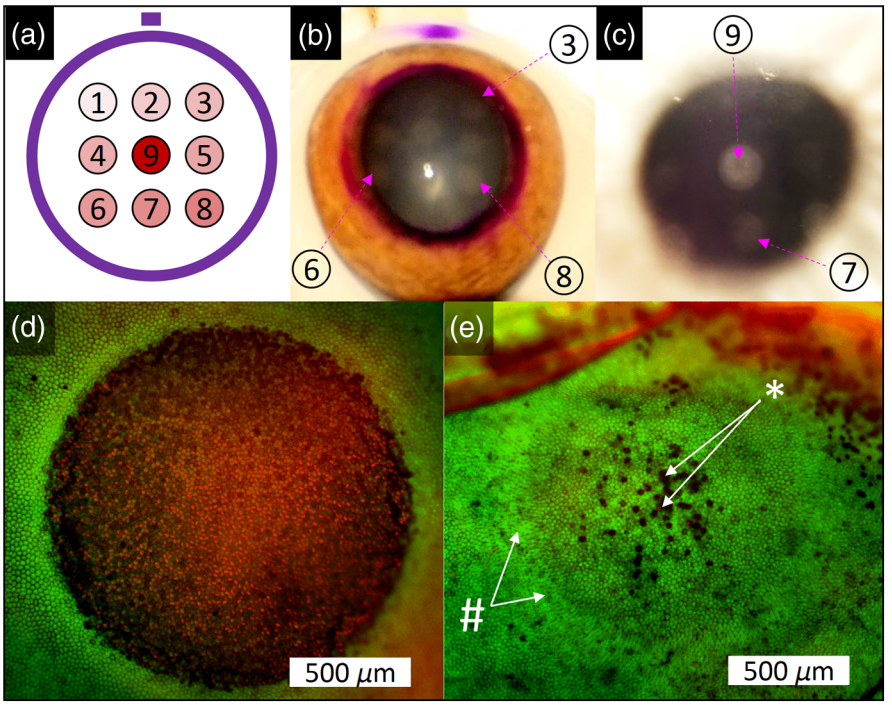

Fig. 2 Evaluation of corneal damage after 355-nm irradiation of enucleated eyes. (a) Diagram of laser exposure pattern. (b) Pig eye at 24 h after laser exposure. Peak cumulative radiant exposures (#1 to 9) in J/cm^2: 50, 100, 200, 300, 400, 500, 600, 1200, and 2400. (c) Rabbit eye at 24 h after laser exposure and injection of toluidine blue into vitreous. Peak cumulative radiant exposures in J/cm^2: 60, 125, 150, 175, 200, 225, 250, 300, and 1200. (d) Live/dead stained pig corneal endothelium with 2400 J/cm^2 lesion, and (e) 200 J/cm^2 lesion.

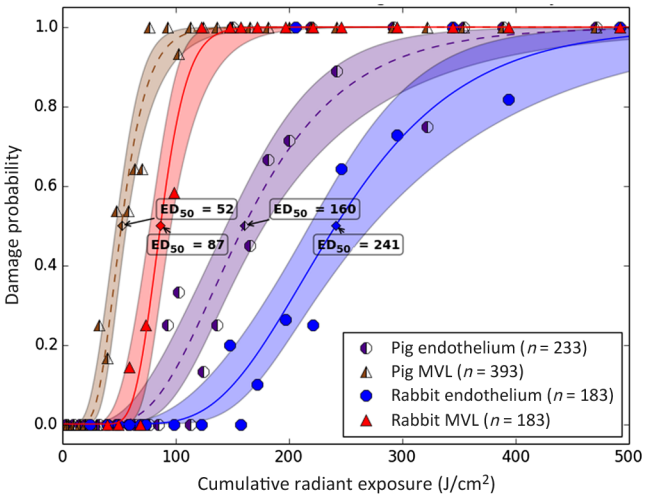

Fig. 3 Probit analysis summary of corneal damage in enucleated pig and rabbit eyes. Data from pig minimum visible lesion (MVL) and endothelial damage are plotted with dotted lines in brown and purple, respectively. Data from enucleated rabbit eyes are plotted with solid lines in red and blue for MVL and endothelial damage, respectively. Shaded areas represent 95% fiducial limit for probit fit.

3.2 *Corneal Damage Threshold with Topical Anesthetics*

The corneal damage threshold after 355-nm exposure was compared after application of two common topical anesthetics: tetracaine and proparacaine. For this comparison, only MVL was used as a damage endpoint and only enucleated pig eyes were tested. The eyes were evaluated both 1 h after laser exposure and after 24 h incubation at room temperature in sealed jars to ensure any damage was noted. The results are shown in Fig. 4 with the corresponding probit fits. The ED_{50} radiant exposure after tetracaine application was very similar to that of pig eyes without topical anesthetic: 50 and 52 J/cm^2, respectively. However, proparacaine application reduced the ED_{50} radiant exposure for detectable lesion to 35 J/cm^2.

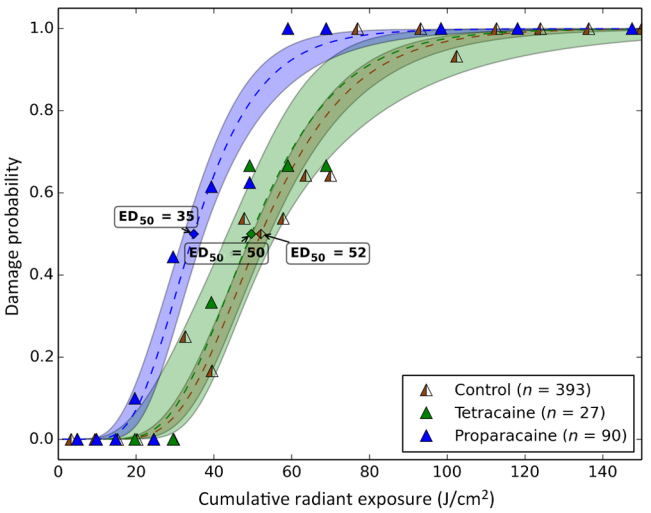

Fig. 4 Probit analysis summary of UV laser-induced corneal damage in enucleated pig eyes after application of balanced saline solution (brown, half-triangles), tetracaine (green), or proparacaine (blue). Dashed line shows probit fit; shaded area indicates 68% fiducial limits.

3.3 *Corneal Damage Threshold in Rabbit Eyes*

Slit lamp analysis of the rabbit eyes was performed in live rabbits under anesthesia, as described above. At the 12- or 48-h time points, the cornea was removed and the endothelium was inspected with live/dead staining. An example of rabbit cornea analysis is shown in Fig. 5. The 12-h slit lamp photo [Fig. 5(a)] shows clearly demarcated opaque lesions, whereas the 48-h image [Fig. 5(b)] shows opacities with more gradual boundaries. Corresponding images of the endothelium after live/dead staining show a patch of missing endothelial cells at 12 h [Fig. 5(c)] with dead stain signal coming from exposed stromal cells. Such an endothelial hole is filled by irregularly shaped cells at 48 h [Fig. 5(d)]. These endothelial changes correspond well to the appearance of the lesions in slit lamp at the same times.

Observation of the corneas under slit lamp over 4 weeks follow-up allowed for assessment of the healing rate of the corneal lesions in rabbits. As shown in Fig. 6 for laser exposures with 0.87- and 1.4-mm beam diameters, only more intense lesions were detectable at longer follow-up times. The radiant exposures corresponding to ED_{50} point for MVL have similar initial (12 h) thresholds for both beam sizes, but with the smaller beam, the thresholds of detectable lesions increased quickly with longer follow-up time, indicating that the smaller beam heals faster. As a result, we used only larger beam data in the probit analysis of MVL and endothelium threshold to guarantee that we were most sensitive to damage. The resulting probit fits in Fig. 7 show ED_{50} of 231 J/cm^2 for MVL ($n = 117$ laser spots) and ED_{50} of 287 J/cm^2 for endothelial damage ($n = 72$ laser spots).

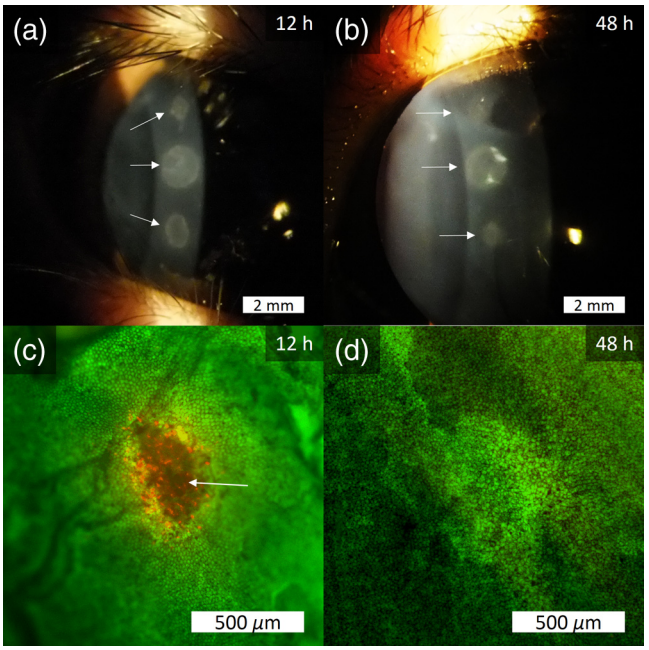

Fig. 5 Evaluation of corneal damage after 355-nm irradiation of rabbit eyes. Slit lamp image of rabbit eye showing second column of exposures with cumulative radiant exposures (top to bottom) of 300, 1200, and 300 J/cm^2 after (a) 12 h and (b) 48 h. Live/dead stained corneal endothelium of 300 J/cm^2 at (c) 12 h and (d) 48 h after laser exposure.

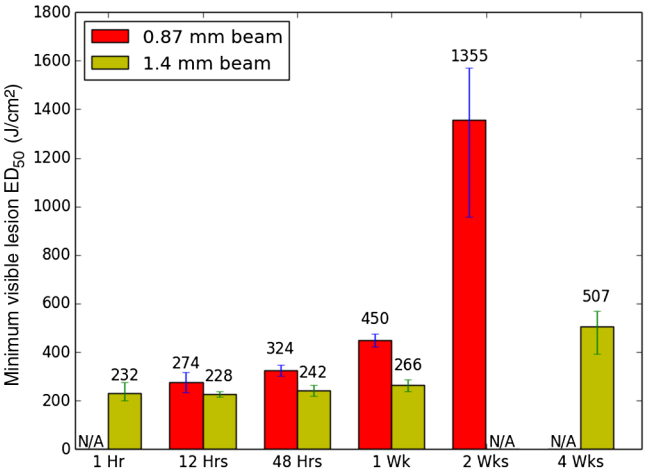

Fig. 6 Healing of corneal damage in rabbits. Bar chart showing ED_{50} damage threshold at different time points with error bars representing 95% fiducial limit.

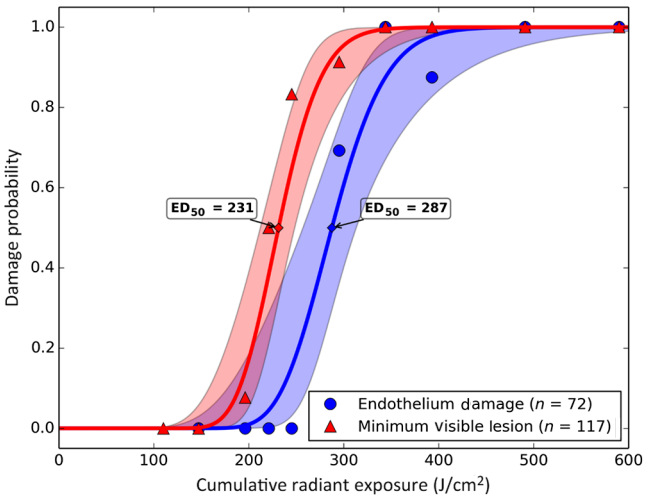

Fig. 7 Probit analysis summary of corneal damage in rabbit eyes. Data from rabbit endothelial damage and MVL damage are plotted with probit fits as solid lines and 95% fiducial limits as the shaded areas.

3.4 *Apoptosis Detection*

TUNEL staining was performed on sections from enucleated porcine eyes and live rabbit eyes to detect apoptotic cells. DAPI was used concurrently to label all nuclei blue, while only apoptotic nuclei are labeled green by the TUNEL staining kit. In both rabbits and pigs, there were no TUNEL-positive cells, except in visible lesions, as identified by slit lamp observation. In addition, TUNEL-positive cells were only seen at radiant exposures that also resulted in endothelial damage. Figure 8 shows TUNEL-stained sections far above the MVL threshold (1200 J/cm^2) and just above the threshold (200 to 300 J/cm^2) for rabbit and pig, respectively. Figure 8(a) illustrates an intense lesion (1200 J/cm^2) in rabbit, with damage throughout all the corneal layers, including a thinned or missing epithelium, apoptotic cells throughout the stroma, and missing endothelial cells. Figure 8(b) shows a threshold lesion (300 J/cm^2) in rabbit with an intact epithelium, seemingly healed by 12 h, apoptotic cells in the anterior stroma, and a

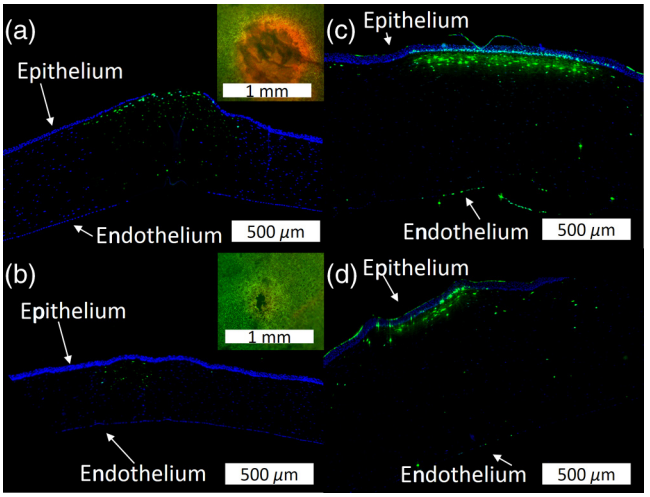

Fig. 8 TUNEL assay of corneal laser lesions in rabbit and enucleated pig eyes. (a) Corneal section from laser lesion (1200 J/cm^2) in rabbit after TUNEL assay. Inset image is an en face view of the endothelium with an equivalent lesion after live/dead staining. (b) Corneal section from laser lesion (300 J/cm^2) in rabbit. (c) Section from laser lesion (1200 J/cm^2) in enucleated pig eye. (d) Section from laser lesion (200 J/cm^2) in pig eye.

mostly intact endothelium. These are consistent with the live/dead staining images from corresponding lesions with the same radiant exposure shown in inset. By contrast, sections from enucleated porcine eyes in Figs. 8(c) and 8(d) show intact epithelium and mostly intact endothelium even at very high radiant exposure. Apoptotic cells are visible in the epithelium, throughout the stroma, and on the endothelium.

3.5 *In Vitro Iris Testing in Pig*

The single-pulse damage threshold for loosely focused nanosecond pulses on the porcine iris was determined by live/dead staining, as shown in Fig. 9. Each line of spots is considered a single data point, where damage is counted if any individual spot shows damage. The probit fit for this data (total of 316 lines delivered) is shown in Fig. 10, where the ED_{50} point is 208 mJ/cm^2.

4 Discussion

4.1 *Corneal Thresholds*

The corneal damage thresholds from enucleated pig eyes support a major assumption of our study that the primary damage

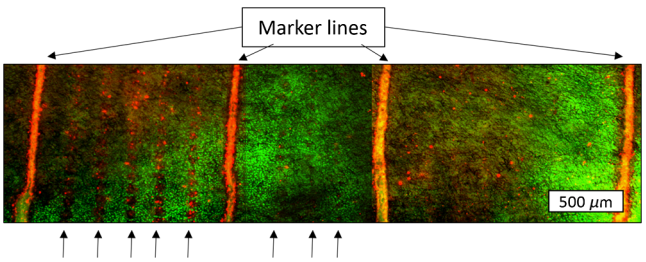

Fig. 9 Live/dead staining of pig iris after scanned 355-nm laser exposure. Radiant exposure of lines from left to right (mJ/cm^2): marker, 960, 840, 720, 600, 480, marker, 360, 240, 180, marker, 150, 120, 90, 60, 30, marker. Last 5 lines were judged as undamaged.

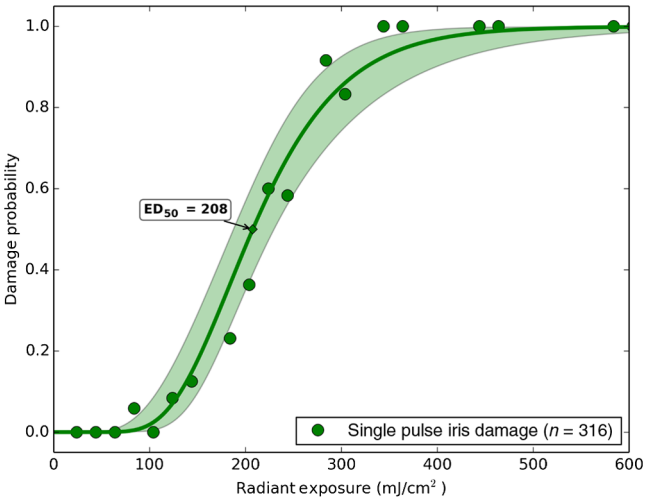

Fig. 10 Probit analysis summary of iris damage in pig eyes. Probit fit for single-pulse iris damage is plotted as the solid line with ED_{50} point of 208 mJ/cm^2. 95% fiducial limits are shown as the shaded area. The zero damage point is 64 mJ/cm^2.

mechanism for 355-nm laser is photochemical. This enucleated pig eye data came from three different configurations for irradiation of porcine corneas with different time-averaged spatial peak irradiances of 26.6 W/cm^2 [Fig. 1(a), $n = 81$], 5.0 W/cm^2 [Fig. 1(b), $n = 180$], and 3.2 W/cm^2 [Fig. 1(c), $n = 132$] with individual pulse exposures of 0.9, 0.16, and 3.2 mJ/cm^2, respectively. Despite this range of irradiances and individual pulse energies, the damage thresholds from the three configurations coincide and are fit neatly by a single probit fit (Fig. 3), suggesting that there are no intensity-dependent thermal effects or other nonlinear effects that contribute to the corneal damage threshold we measure.

The collected corneal damage thresholds derived from probit fits of the measurements in live rabbit, donor human eyes, enucleated rabbit and porcine eyes are listed in Table 1 along with probit slopes and zero damage points, which represent the highest experimentally observed exposures with no damage. From this table, it is clear that the MVL method of damage assessment is more sensitive than endothelial damage for all species. This might be due to the fact that the epithelium and stroma receive up to 30% higher dose of UV radiation than the endothelium due to absorption. This hypothesis is supported by the larger ratio between MVL and endothelium thresholds in enucleated pig eyes, which have thicker cornea (666 μm[16]) than in rabbit eyes (300- to 400-μm thick cornea[17]). Pitts et al.[10] also noted this trend and reported epithelial damage at the lowest radiant exposure and stromal opacities and endothelial changes appearing at progressively higher radiant exposures. This observation is advantageous for evaluating clinical safety since MVL is a simpler damage assessment than endothelial methods, such as cell counting. Since the epithelium is rapidly healing and has a lower damage threshold than that of the endothelium, it will serve as a first and safe indicator of potential corneal damage in clinical trials, thereby providing safeguards against irreparable damage to the endothelium.

The fact that corneal damage thresholds in enucleated eyes are lower than the thresholds *in-vivo*, as seen by comparing the thresholds for rabbit eyes, may indicate the presence of natural UV protective mechanisms, which inhibit DNA damage in live eyes. For example, ferritin, an iron-binding complex, is known to inhibit UV-induced oxidative damage to DNA in corneal epithelial cells.[18] A similar compound, lactoferrin, is a component

Table 1 Table of damage thresholds with fit parameters. The "zero damage" point represents the last experimental radiant exposure with no damage is shown in the last column.

Tissue type	*In vivo*/ *ex vivo*	Damage criteria	ED_{50} threshold	Threshold exposure duration	95% fiducial to ED_{50}	Slope (ED_{84}/ED_{50})	Zero damage point
Rabbit cornea	*In vivo*	Visible lesion	231 J/cm^2	46 s	212 to 248 J/cm^2	1.16	147 J/cm^2
		Endothelium live/ dead	287 J/cm^2	57 s	257 to 313 J/cm^2	1.17	245 J/cm^2
Rabbit cornea	*Ex vivo*	Visible lesion	87 J/cm^2	17 s	77 to 96 J/cm^2	1.24	49 J/cm^2
		Endothelium live/ dead	241 J/cm^2	48 s	218 to 273 J/cm^2	1.44	123 J/cm^2
Human cornea	*Ex vivo*	Visible lesion	110 J/cm^2	22 s	86 to 162 J/cm^2	1.31	49 J/cm^2
		Endothelium live/ dead	453 J/cm^2	90 s	378 to 676 J/cm^2	1.22	350 J/cm^2
Pig cornea	*Ex vivo*	Visible lesion	52 J/cm^2	10 s[a]	47 to 57 J/cm^2	1.41	29 J/cm^2
		Endothelium live/ dead	160 J/cm^2	32 s[a]	145 to 178 J/cm^2	1.54	85 J/cm^2
Pig cornea (with proparacaine)	*Ex vivo*	Visible lesion	35 J/cm^2	7 s	29 to 41 J/cm^2	1.46	15 J/cm^2
Pig iris	*Ex vivo*	Live/dead staining	208 mJ/cm^2	0.8 ns	187 to 230 mJ/cm^2	1.42	64 mJ/cm^2

[a]For setup in Fig. 1(b), where most of the data were collected.

of tears[19] and is removed during enucleation and storage. The localization of these compounds in the corneal epithelium may also explain why the MVL threshold, which is sensitive to epithelial and stromal damage, is affected more significantly by enucleation than the endothelial threshold. Thus, while postmortem eyes are a convenient model for ophthalmic applications, they may overestimate the hazard from UV radiation to the cornea.

Comparison of our damage thresholds assessed by MVL to the two previous studies by Pitts et al.[10] and Zuclich et al.[12] and to the current safety standards is shown in Fig. 11. It is clear that our *in-vivo* results are significantly higher than in previous damage threshold studies. Comparing to the study of Pitts et al.,[10] the major difference is the UV source (Xe–Hg lamp) and duration of exposure. For 365 nm, the threshold exposure was more than 4.5 h for a cumulative radiant exposure of 42.5 J/cm^2 while our threshold exposures correspond to 46 s. Two possible factors for the large discrepancy are additional damage from corneal drying during the lengthy exposure and potential leakage of shorter, more lethal, wavelengths from the UV lamp. The study of Zuclich[12] offers an even more direct comparison with similar laser wavelengths and exposure durations, but a different animal model (rhesus monkeys). Even after adjusting their values to peak radiant exposure rather than average radiant exposure (factor of 2), our values remain 40% to 75% higher for similar wavelengths. It should be noted that the study of Zuclich[12] was done with a continuous-wave laser (Argon-ion) or long-pulsed at 50% duty cycle (Krypton-ion), while our experiment was performed with short-pulsed lasers with much lower duty cycle (1.65E-5). Nevertheless, we believe that the corneal damage thresholds are photochemical in nature, and thus, cumulative radiant exposure is the key value to compare. Our results with enucleated eyes from three different species indicate that there is some variation between species in corneal susceptibility, which may account for this discrepancy. While the number of human donor eyes used in this study was limited, the results suggest that human eyes are not more susceptible to damage from 355-nm laser than rabbits. Thus, the *in-vivo* rabbit thresholds are a reasonable reference point for 355-nm laser thresholds during surgical procedures in humans.

Looking at the safety standards, it is clear that there is a significant safety margin between the damage threshold and the standards. The International Commission on Non-Ionizing Radiation Protection 2004 guidelines gave a safety limit of 19 J/cm^2 (averaged over 1-mm diameter aperture) for 355-nm radiation[20] based on the potential for photochemical damage to the cornea. This was revised to a far more conservative value, 1 J/cm^2, for all UVA wavelengths (315 to 400 nm) in the 2005 adjustment[21] and 2013 guidelines[22] based on the potential for thermal cataractogenesis. Our damage threshold of 231 J/cm^2 in rabbits and the experimental no-damage limits of 147 J/cm^2 in rabbits and 29 J/cm^2 in pig eyes suggest that this value is very conservative.

4.2 *Effect of Topical Anesthetics*

Our measurement on enucleated pig eyes with tetracaine and proparacaine showed very surprising results. Although the two common anesthetics are derivatives of para-aminobenzoic acid and used to inhibit sodium ion channels, proparacaine showed a reduction in the MVL threshold, whereas tetracaine did not. Both local anesthetics are known to damage the corneal epithelium following excessive use and they may do so by altering cell membranes, cytoskeleton, and metabolism.[23] Further testing is required to understand why proparacaine, which was shown to be less toxic in equal concentration to tetracaine,[23] lowers the UV damage threshold, while tetracaine does not. The possibility of a cytotoxic interaction between the laser and this or other ophthalmic solutions is one that should be carefully considered during development of clinical laser applications.

4.3 *Iris Thresholds*

There are several early reports of laser damage to the iris, including one from Watts,[14] who used a ruby laser at 693.4 nm and saw "destruction" beginning at an energy density of 1.1 J/cm^2. However, insufficient iris laser damage measurements, particularly for shorter pulses, means that the 2014 ANSI Z136.1 iris safety limit must be extrapolated as 5× the skin limit for wavelengths between 400 and 1400 nm.[24] Since the iris absorbs all of

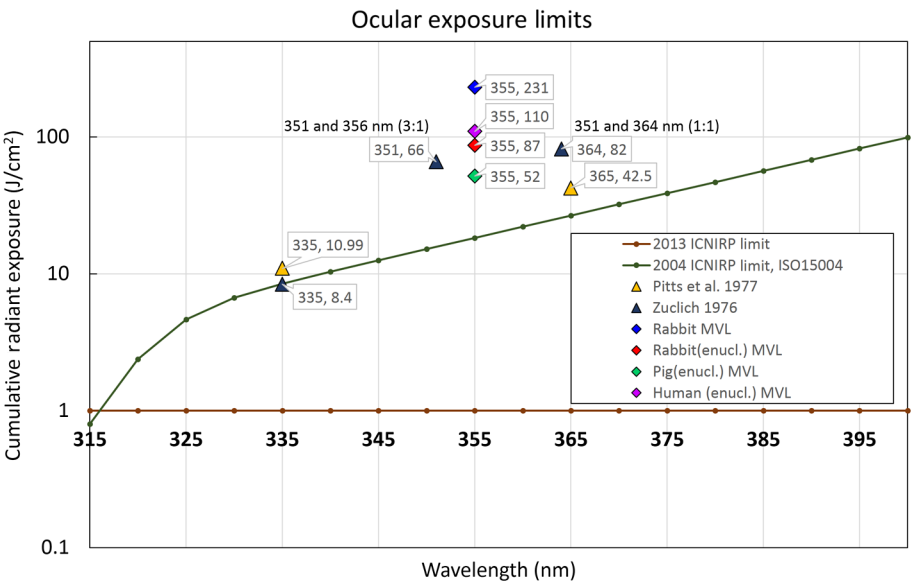

Fig. 11 Comparison between experimental results and safety standards.

355 nm as well as 400 nm, we apply this standard to our laser parameters (0.8 ns) and derive a single-pulse radiant exposure limit of 14.8 mJ/cm^2. Our measured ED_{50} of 208 mJ/cm^2 is more than 14× this safety limit. While it is unlikely that standard refractive patterns will approach this value on the iris, this result adds another data point to guide the use of 355 nm in ocular applications.

5 Conclusions

For detection of photochemical corneal damage by 355-nm subnanosecond lasers, visible lesion observation is the more sensitive measure compared to endothelial changes or apoptosis. The median effective dose for visible lesions on rabbit corneas *in-vivo* was measured to be 231 J/cm^2, while endothelial damage occurred at 287 J/cm^2. The experimental no-damage point on rabbit corneas was 150 J/cm^2, which exceeds the corneal exposure during 355-nm LASIK flap cutting by more than a factor of 20.[4] These values suggest that corneal damage thresholds are high enough to motivate further development of 355-nm subnanosecond lasers as a replacement for near-infrared femtosecond lasers in LASIK and other ophthalmic surgeries.

Acknowledgments

The authors would like to thank David Dewey for ANSI safety calculations. Funding was provided by the U.S. Air Force Office of Scientific Research (Grant No. FA9550-10-1-0503) and the Stanford Photonics Research Center.

References

1. T. Juhasz et al., "Corneal refractive surgery with femtosecond lasers," *IEEE J. Sel. Top. Quantum Electron.* **5**(4), 902–910 (1999).
2. M. Q. Salomão and S. E. Wilson, "Femtosecond laser in laser in situ keratomileusis," *J. Cataract Refract. Surg.* **36**(6), 1024–1032 (2010).
3. P. S. Binder, "Femtosecond applications for anterior segment surgery," *Eye Contact Lens* **36**(5), 282–285 (2010).
4. A. Trost et al., "A new nanosecond UV laser at 355 nm: early results of corneal flap cutting in a rabbit model," *Investig. Ophthalmol. Vis. Sci.* **54**(13), 7854–7864 (2013).
5. A. Vogel, S. Freidank, and N. Linz, "Alternatives to femtosecond laser technology: subnanosecond UV pulse and ring foci for creation of LASIK flaps," *Ophthalmologe* **111**(6), 531–538 (2014).
6. D. Z. Reinstein, T. J. Archer, and M. Gobbe, "Small incision lenticule extraction (SMILE) history, fundamentals of a new refractive surgery technique and clinical outcomes," *Eye Vis.* **1**(1), 3 (2014).
7. T. Liu et al., "Comparative study of corneal endothelial cell damage after femtosecond laser assisted deep stromal dissection," *Biomed. Res. Int.* **2014**, 1–10 (2014).
8. D. V. Palanker et al., "Femtosecond laser-assisted cataract surgery with integrated optical coherence tomography," *Sci. Transl. Med.* **2**(58), 58ra85 (2010).
9. J. van de Kraats and D. van Norren, "Optical density of the aging human ocular media in the visible and the UV," *J. Opt. Soc. Am. A* **24**(7), 1842 (2007).
10. D. G. Pitts, A. P. Cullen, and P. D. Hacker, "Ocular effects of ultraviolet radiation from 295 to 365 nm," *Invest. Ophthalmol. Vis. Sci.* **16**(10), 932–939 (1977).
11. J. A. Zuclich, "Ultraviolet-induced photochemical damage in ocular tissues," *Health Phys.* **56**(5), 671–682 (1989).
12. J. A. Zuclich and J. S. Connolly, "Ocular damage induced by near-ultraviolet laser radiation," *Invest. Ophthalmol. Vis. Sci.* **15**(9), 760–764 (1976).
13. H. Sun, R. M. Kurtz, and T. Juhasz, "Finite element model of the temperature increase in excised porcine cadaver iris during direct illumination by femtosecond laser pulses," *J. Biomed. Opt.* **17**(7), 078001 (2012).
14. G. K. Watts, "Retinal hazards during laser irradiation of the iris," *Br. J. Ophthalmol.* **55**(1), 60–67 (1971).
15. G. Schuele et al., "RPE damage thresholds and mechanisms for laser exposure in the microsecond-to-millisecond time regimen," *Invest. Ophthalmol. Vis. Sci.* **46**(2), 714–719 (2005).
16. C. Faber et al., "Corneal thickness in pigs measured by ultrasound pachymetry *in vivo*," *Scand. J. Lab. Anim. Sci.* **35**(1), 39–43 (2008).
17. A. Gwon, "The rabbit in cataract/IOL surgery," in *Animal Models in Eye Research*, P. A. Tsonis, Ed., pp. 184–204, Elsevier Ltd., San Diego, California (2008).
18. C. X. Cai, D. E. Birk, and T. F. Linsenmayer, "Nuclear ferritin protects DNA from UV damage in corneal epithelial cells," *Mol. Biol. Cell* **9**, 1037–1051 (1998).
19. S. Shimmura et al., "Subthreshold UV radiation-induced peroxide formation in cultured corneal epithelial cells: the protective effects of lactoferrin," *Exp. Eye Res.* **63**, 519–526 (1996).
20. The International Commission on Non-Ionizing Radiation Protection, "Guidelines on limits of exposure to ultraviolet radiation of wavelengths between 180 nm and 400 nm (incoherent optical radiation)," *Health Phys.* **87**(2), 171–186 (2004).
21. D. Sliney et al., "Adjustment of guidelines for exposure of the eye to optical radiation from ocular instruments: statement from a task group of the International Commission on Non-Ionizing Radiation Protection (ICNIRP)," *Appl. Opt.* **44**(11), 2162 (2005).
22. "ICNIRP guidelines on limits of exposure to laser radiation of wavelengths between 180 nm and 1,000 m," *Health Phys.* **105**(3), 271–295 (2013).
23. R. L. Grant and D. Acosta, "Comparative toxicity of tetracaine, proparacaine and cocaine evaluated with primary cultures of rabbit corneal epithelial cells," *Exp. Eye Res.* **58**(4), 469–478 (1994).
24. Laser Institute of America, "American National Standard for Safe Use of Lasers," ANSI Z136.1-2014, Orlando, Florida (2014).

Jenny Wang received her AB degree in chemistry and physics from Harvard College in 2010. She is currently pursuing a PhD in applied physics from Stanford University working on laser-tissue interactions in ophthalmic surgery.

Jae Lim Chung is currently a professor at Kim's Eye Hospital, Department of Ophthalmology, Konyang University College of Medicine, Seoul, Republic of Korea. His professional interests are corneal disease, ocular infectious disease, dry eye disease, ophthalmic lasers, cataract, and refractive surgery. He was a visiting scholar of the Department of Ophthalmology and Hansen Experimental Physics Laboratory at Stanford University.

Daniel Palanker is a professor in the Department of Ophthalmology and in the Hansen Experimental Physics Laboratory at Stanford University. He is working on optical and electronic technologies for imaging, diagnostic, therapeutic, surgical and prosthetic applications, primarily in ophthalmology. These studies include laser-tissue interactions with applications to nondamaging laser therapy and surgery with ultrafast lasers, retinal prosthetics for restoration of sight, electronic control of organs, as well as interferometric imaging of neural signals.

Biographies for the other authors are not available.